Supplementary Information

Two-inch wafer-scale manufacturing of Micro-QLED for AR microdisplay application

Yuyu Jing[1], Mingyu Yao[1], Chen Zhang[2,3], Junhua Kuang[1], Weibin Li[2,3 +], Yuren Wang[2,3], Haizheng Zhong[1 *]

1 MIIT Key Laboratory for Low-Dimensional Quantum Structure and Devices, School of Materials Science and Engineering, Beijing Institute of Technology, Beijing 100081, China

2 National Microgravity Laboratory, Institute of Mechanics, Chinese Academy of Sciences, 100190 Beijing, China

3 School of Engineering Science, University of Chinese Academy of Sciences, 100049 Beijing, China

* hzzhong@bit.edu.cn

[+] liweibin@imech.ac.cn

Supplementary Table S1. Performance comparison with reported large-area QLED and PeLED devices.

Method	Material	Solvent engineering	Color	Active electroluminescence area / mm^{-2}	peak EQE	EL pixel size	Ref.
Spin coating	CdSe	octane and hexane	R, G	1600	R 22.8 % G 20.8% B 1.4%	10 μm 4×12 μm 10 μm	This work
Spin coating	CdSe	octane and hexane	R, G	1600	R 19.7 % G 16.6%	N/A	This work
Spin coating	CdSe	octane	R	4	R 20.5 %	N/A	1
Spin coating	CdSe	octane	B	4	21.6%	N/A	2
Brush coating direct writing	CdSe	octane	R, G, B	4	R 18.96% G 17.40% B 6.2%	N/A	3
Brush coating direct writing	CdSe	octane	R, G, B	400 324 332	R 20.49% G 13.72% B 7.57%	N/A	4
Blade coating	CdSe	octane	R	4 625	12.48% NA	N/A	5
Blade coating	CdSe	octane	R	400	21.8%	N/A	6
Electrophoretic deposition	CdSe	octane	R, G, B	4 10000	N/A、 N/A	N/A	7
Spin coating	$FAPbBr_3$ nanocrystals	hexane	G	400	16%	N/A	8
Spin coating	quasi-2D perovskite	DMSO solvent	G	900	16.4%	N/A	9
Blade-coating	$CsPb(Br_{0.84}Cl_{0.16})_3$ 2D perovskite	DMSO/DMF solvent	B	4 2800	10.3% N/A	N/A	10
Inkjet Printing	$FA_{0.8}Cs_{0.2}PbI_3$ 2D perovskite	DMSO/DMF solvent	R	4 2800	14.3% N/A	N/A	11
Blade-coating	$CsPbI_3$ QDs	octane and hexane	R R	4 2800	15.3% N/A	N/A	12

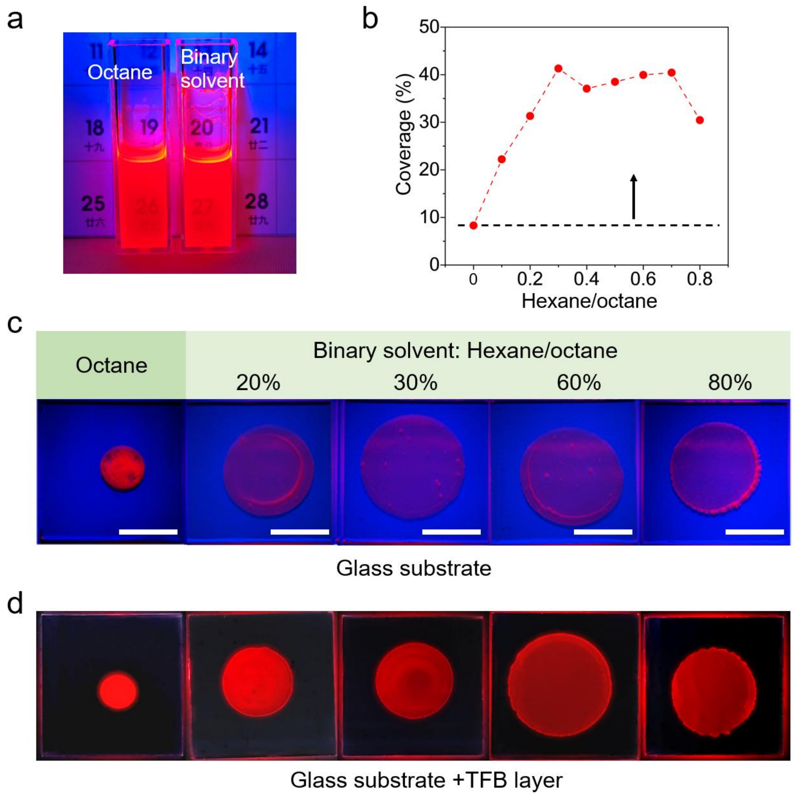

Supplementary Fig. S1 (a) QD inks in n-octane and binary solvents of n-hexane/n-octane. (b) Statistical coverage ratio of QD films on the glass substrate. (c) Spreading area evaluation on glass substrates with different binary solvents ratios (the volume of droplet is 3 μL). (d) Spreading area evaluation on TFB layer with different binary solvents ratios (the volume of droplet is 3 μL).

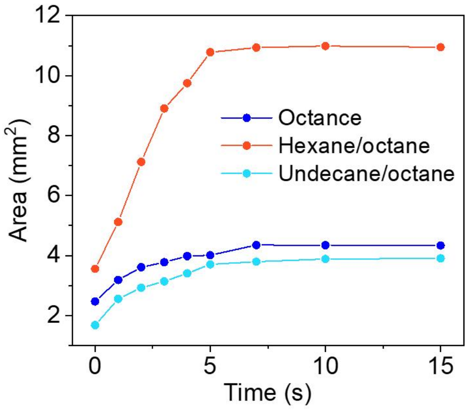

Supplementary Fig. S2 The spreading area versus time using n-octane system, binary solvents of n-hexane/n-octane system and binary solvents of undecane/n-octane system.

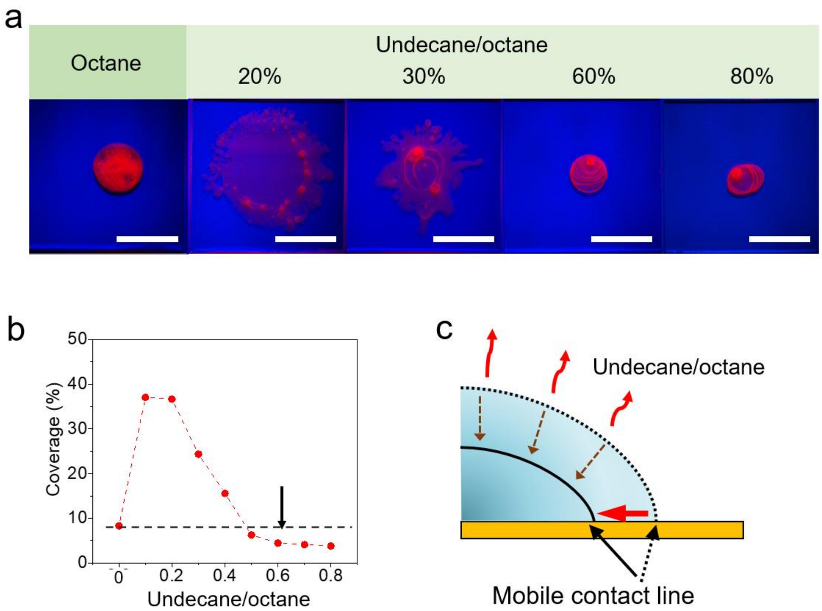

Supplementary Fig. S3 (a) Spreading area evaluation on glass substrates with different binary solvents of undecane/n-octane (the volume of droplet is 3 μL). (b) Statistical coverage ratio of QD films. (c) Schematic diagram for the mobile three phase contact line of binary solvents of undecane and octane system.

Supplementary Fig. S4 In situ microscopy observation of QDs droplet spreading process using binary solvents of undecane/n-octane system. The volume of QD droplet is 0.2 μL. Stacked video frames from 0 s to 5 s to show the spreading tracks of QD droplet.

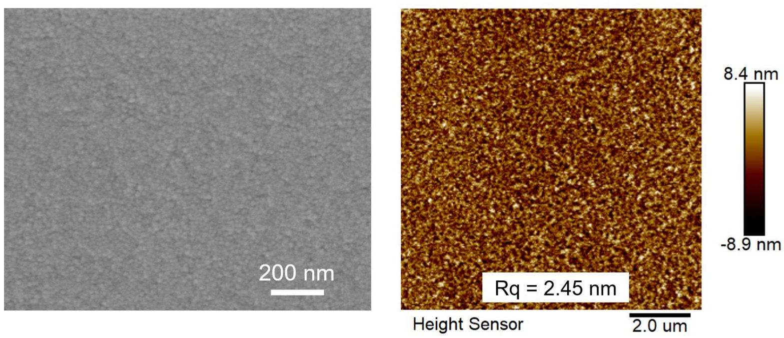

Supplementary Fig. S5 SEM and AFM images of spin-coated QD films with the n-hexane/n-octane volume ratio of 60%, respectively.

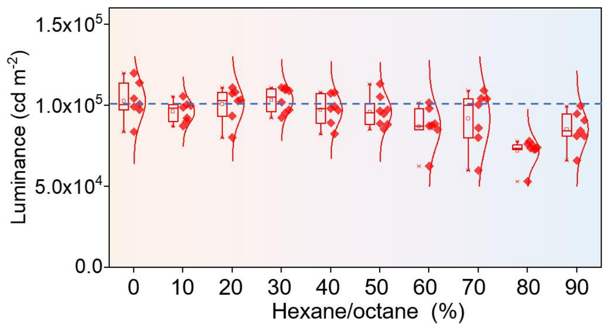

Supplementary Fig. S6 Luminance of multiple QLED devices with different n-hexane/n-octane volume ratio from 0 to 90%. The standard deviation of the data collected from >6 samples.

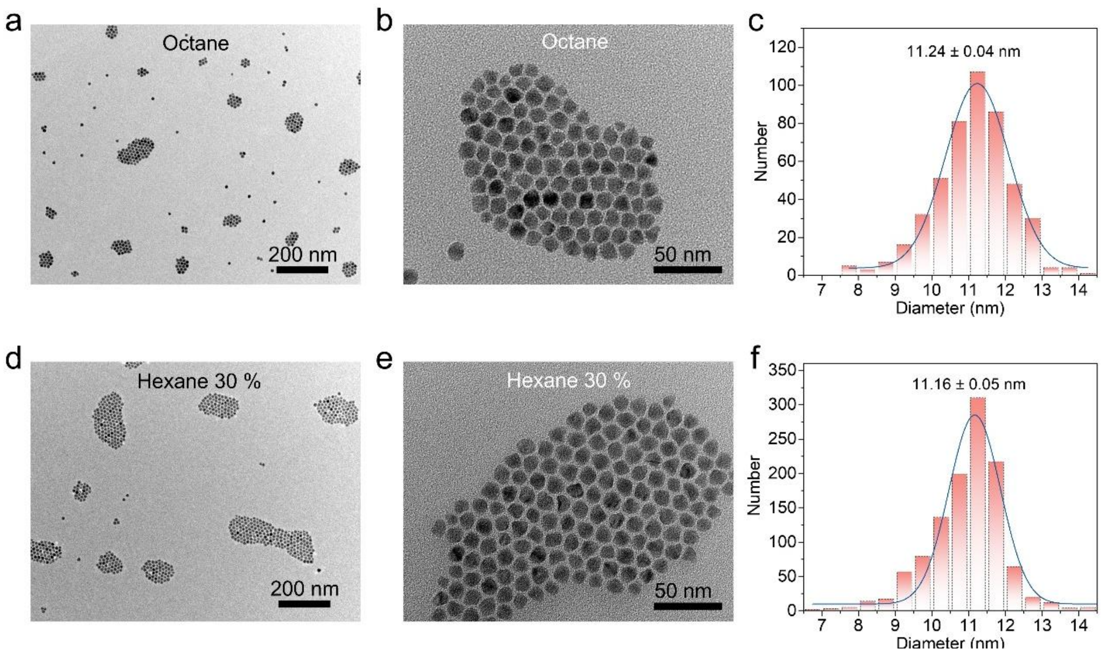

Supplementary Fig. S7 Characterization of QDs dispersed in n-octane and in a 30% n-hexane/n-octane binary solvent. (a) (b) TEM images of QDs dispersed in n-octane and (c) corresponding size distribution with an average diameter of 11.24 ± 0.04 nm. (d) (e)TEM images of QDs dispersed in 30% n-hexane/n-octane binary solvent and (f) corresponding size distribution with an average diameter of 11.16 ± 0.05 nm.

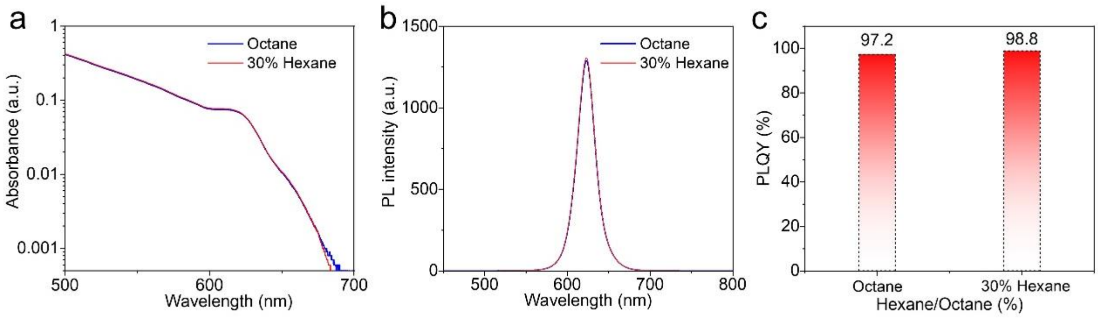

Supplementary Fig. S8 Optical properties of QDs dispersed in n-octane and in a 30%

n-hexane/n-octane binary solvent. (a) Absorption spectra, (b) Photoluminescence (PL) spectra, and (c) corresponding PL quantum yields (PLQY).

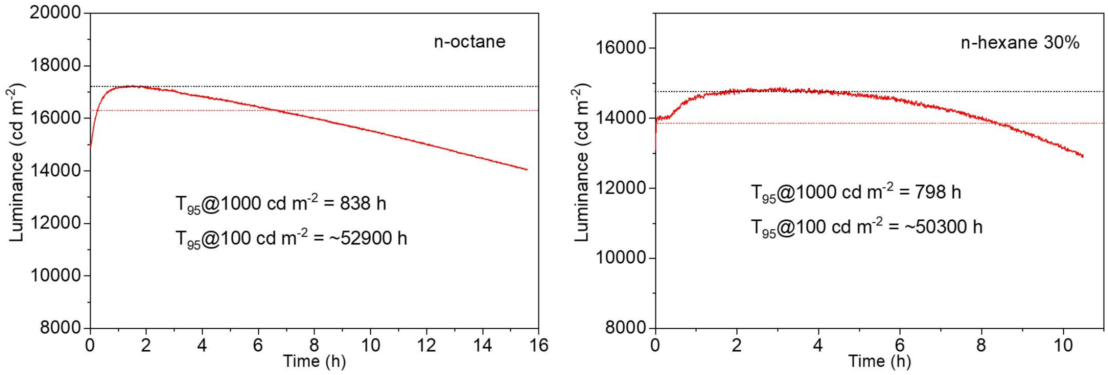

Supplementary Fig. S9 Operational lifetimes of QLEDs based different n-hexane/n-octane volume ratio of 0 and 30%. Luminance as a function of operational time.

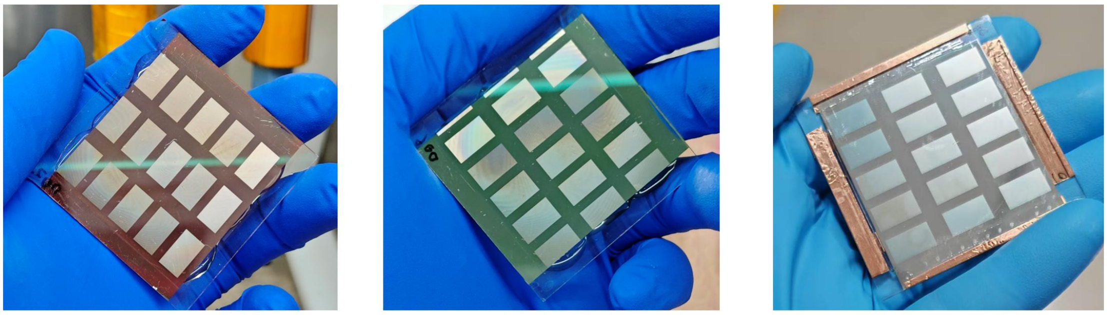

Supplementary Fig. S10 Images of 2-inch red, green and blue emitting Micro-QLED devices.

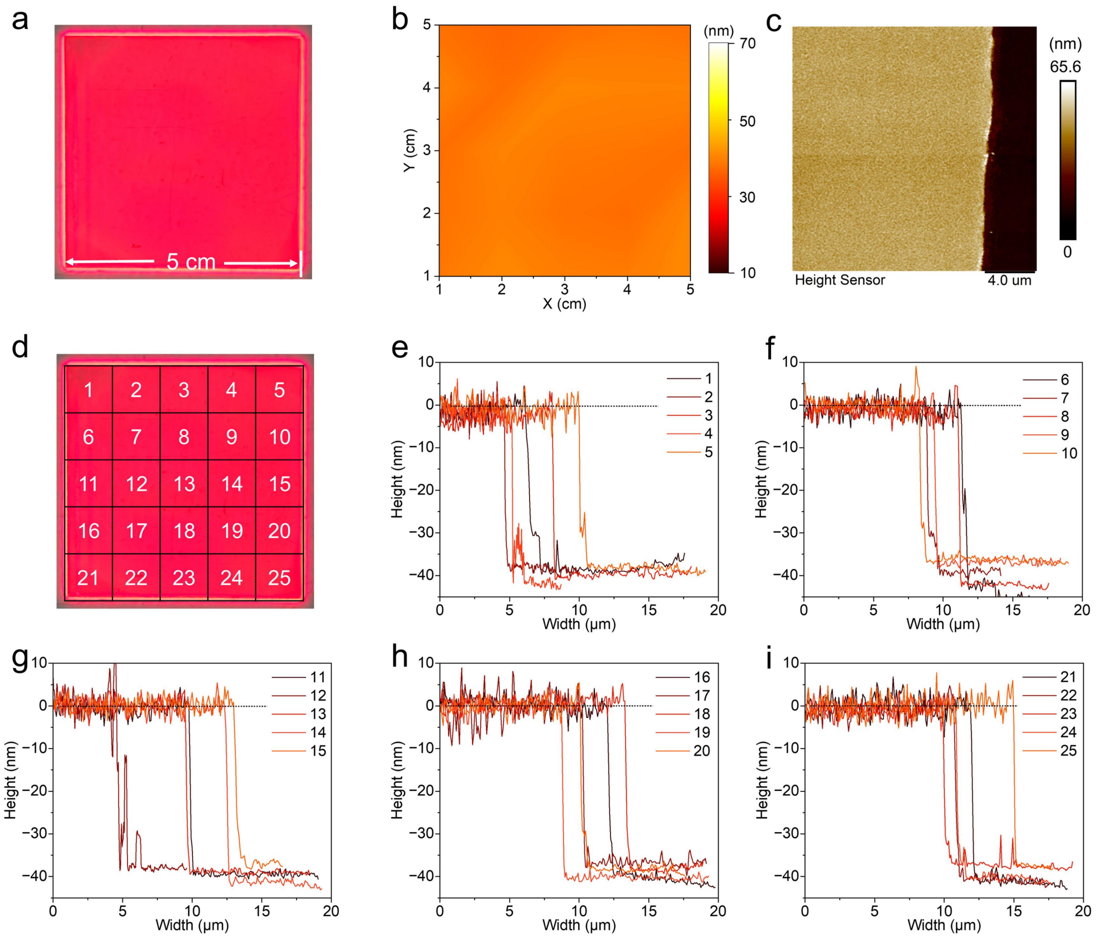

Supplementary Fig. S11 Characterization of the 2-inch red QD films fabricated with the QD ink of binary solvent 30% n-hexane. (a) PL images, (b) Thickness mapping and (c) AFM images of 2-inch red QD films. (d) Schematic diagram of measurement area for AFM images. (b-f) Height profiles of QD films.

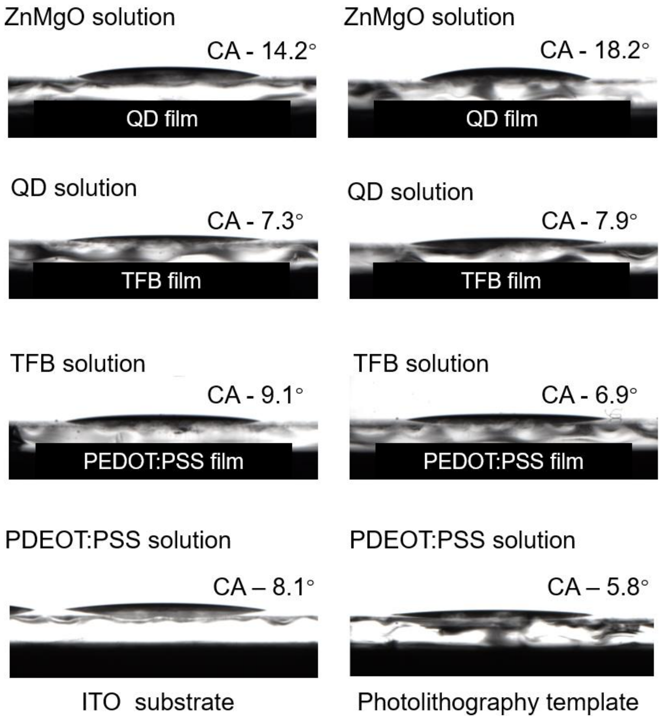

Supplementary Fig. S12 Contact angle of photolithography template and the pristine ITO substrate.

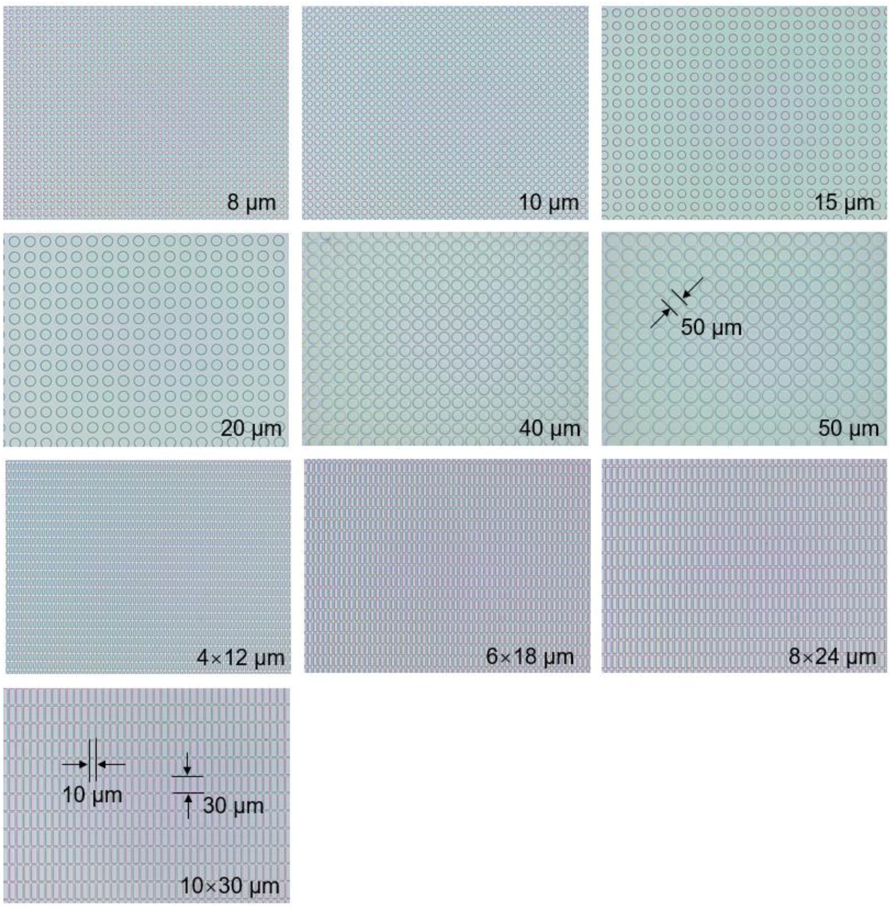

Supplementary Fig. S13 Photolithography templates of different sizes from 50 μm to 4 μm.

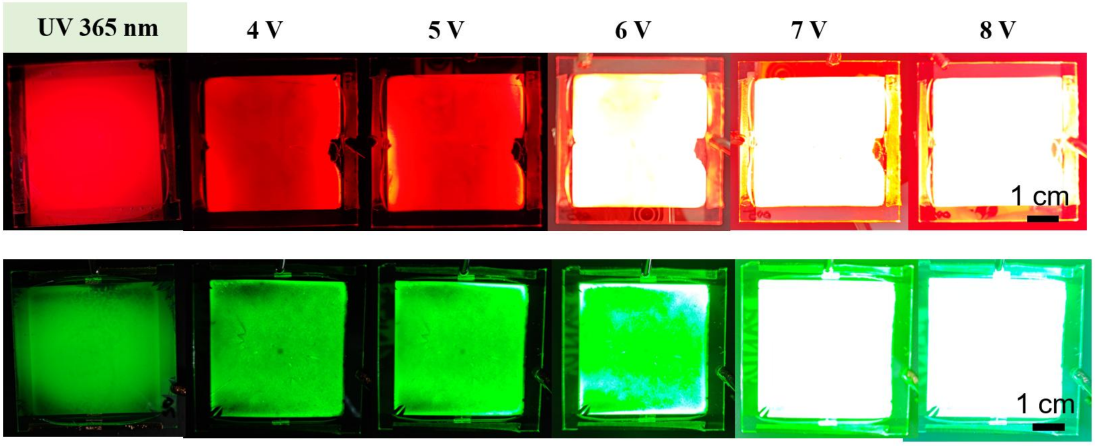

Supplementary Fig. S14 Electroluminescence images of 2-inch red and green QLED devices under the increased driving voltages.

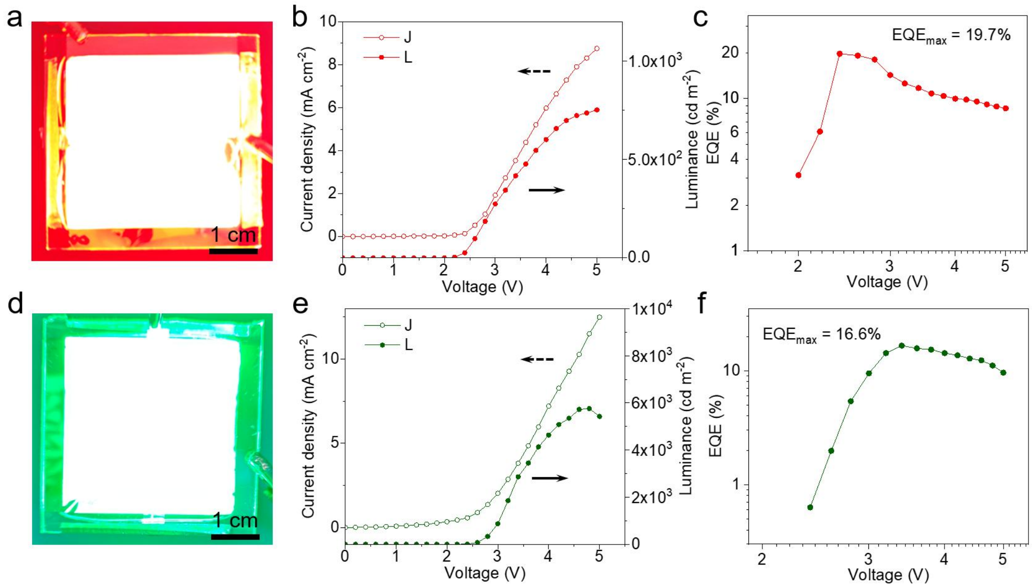

Supplementary Fig. S15 Device performance of 2-inch QLED. (a) Electroluminescence images of red patterned QLED device. Scale bar, 1 cm. (b) Current density-voltage-luminance curves and (c) EQEs versus voltage of red-emitting 2-inch QLED. (d) EL images of green patterned QLED device. Scale bar, 1 cm. (e) J-V-L curves and (f) EQEs versus voltage of green-emitting 2-inch QLED.

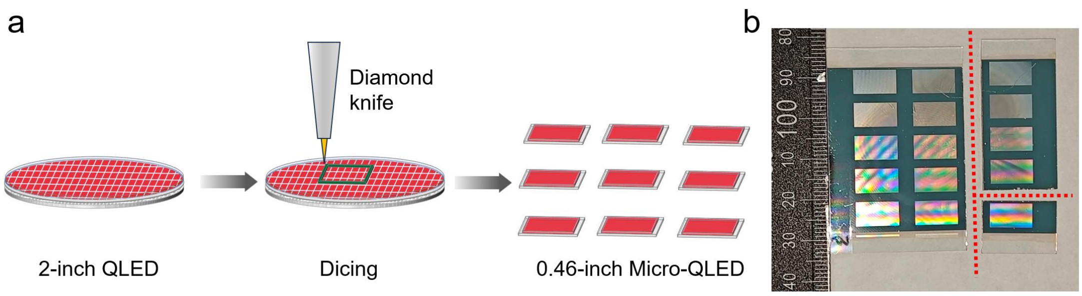

Supplementary Fig. S16 Schematic diagram for the dicing process of 2-inch Micro-QLED device

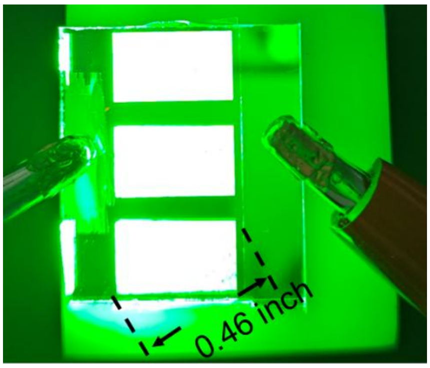

Supplementary Fig. S17 EL images of multiple 0.46-inch Micro-QLED panels.

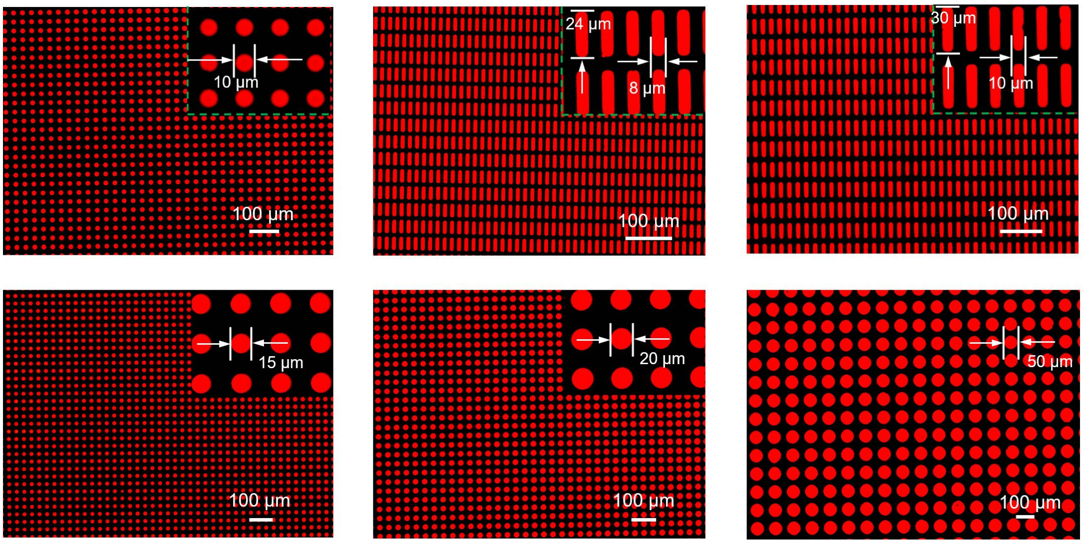

Supplementary Fig. S18 Electroluminescence optical microscopy images of red patterned Micro-QLED device.

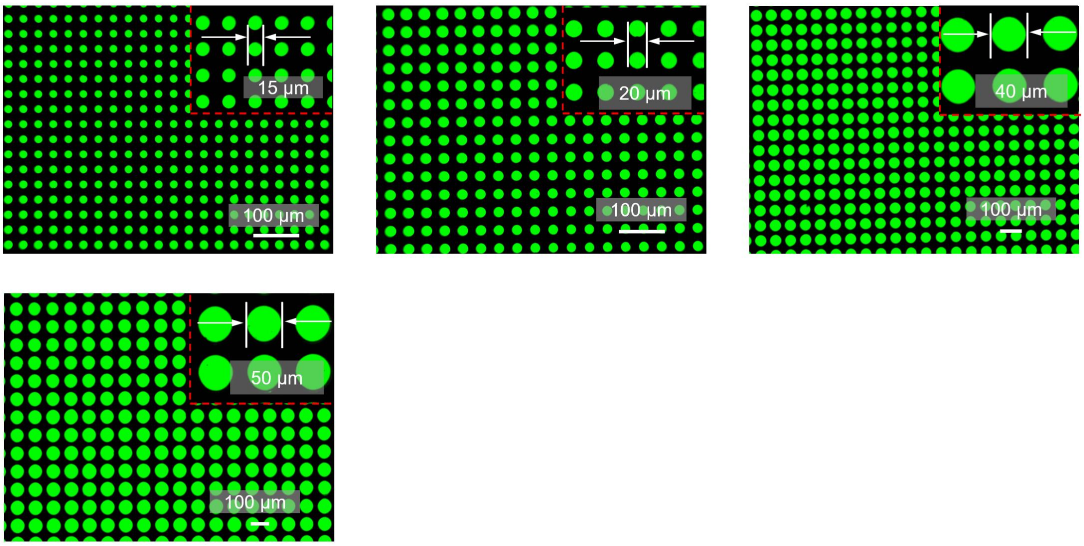

Supplementary Fig. S19 Electroluminescence optical microscopy images of green patterned Micro-QLED device.

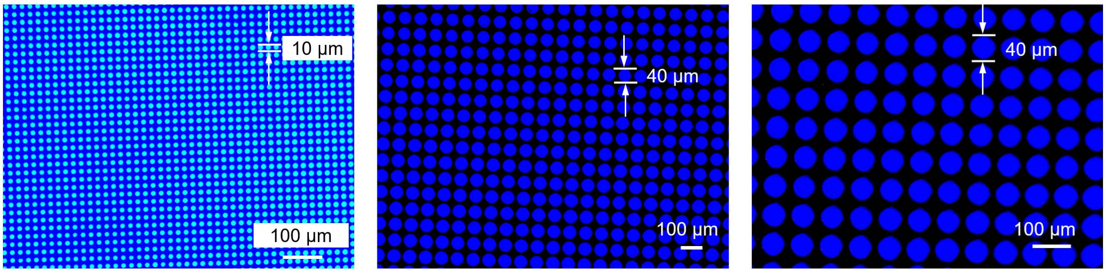

Supplementary Fig. S20 Electroluminescence optical microscopy images of blue patterned Micro-QLED device.

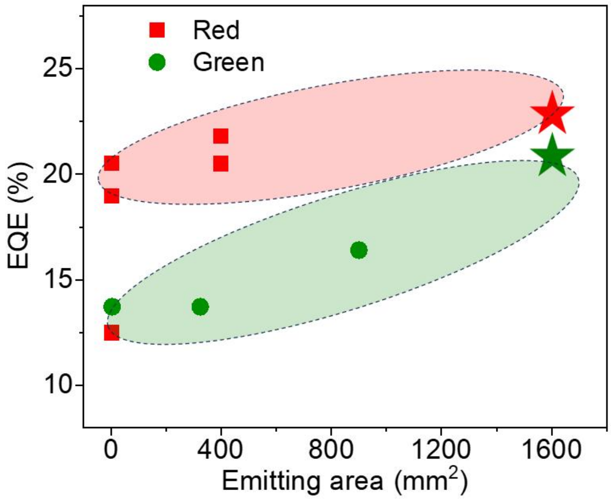

Supplementary Fig. S21 Comparison of large-area QLED performance including EQEs and active emitting area in this work (five-pointed star) and other reported works.

References

1. Dai X. L. et al. Solution-processed, high-performance light-emitting diodes based on quantum dots. *Nature* **515,** 96-99 (2014).
2. Jin W. X. et al. Water-induced high-performance quantum-dot light-emitting diodes. *Nature Photonics* **19,** 1233–1239 (2025).
3. Zhang M. et al. Ultrasmooth Quantum Dot Micropatterns by a Facile Controllable Liquid-Transfer Approach: Low-Cost Fabrication of High-Performance QLED. *Journal of the American Chemical Society* **140,** 8690-8695 (2018).
4. Zhang M. et al. Direct Writing Large-Area Multi-Layer Ultrasmooth Films by an All-Solution Process: Toward High-Performance QLEDs. *Angewandte Chemie International Edition* **60,** 680-684 (2021).
5. Yu H. W. et al. Efficient All-Blade-Coated Quantum Dot Light-Emitting Diodes through Solvent Engineering. *The Journal of Physical Chemistry Letters* **11,** 9019-9025 (2020).
6. Yu H. W. et al. High-Efficiency, Large-Area, Flexible Top-Emitting Quantum-Dot Light-Emitting Diode. *ACS Photonics* **10,** 2192-2200 (2022).
7. Zhao J. Y. et al. Large-area patterning of full-color quantum dot arrays beyond 1000 pixels per

inch by selective electrophoretic deposition. *Nature Communications* **12,** 4603 (2021).
8. Wang H. R. et al. A Multi-functional Molecular Modifier Enabling Efficient Large-Area Perovskite Light-Emitting Diodes. *Joule* **4,** 1977-1987 (2020).
9. Sun C. J. et al. High-performance large-area quasi-2D perovskite light-emitting diodes. *Nature Communication* **12,** 2207 (2021).
10. Chu S. et al. Large-Area and Efficient Sky-Blue Perovskite Light-Emitting Diodes via Blade-Coating. *Advanced Materials* **34,** e2108939 (2022).
11. Liu H. et al. Large-Area Flexible Perovskite Light-Emitting Diodes Enabled by Inkjet Printing. *Advanced Materials* **36,** e2309921 (2024).
12. Shi G. et al. Manipulating solvent fluidic dynamics for large-area perovskite film-formation and white light-emitting diodes. *Nat Commun* **15,** 1066 (2024).